Royal Netherlands Institute for Sea Research

This is a postprint of:

Kim, Y.-H., Buscail, R., Fanget, A.-S., Eyrolle-Boyer, F., Bassetti, M.-A., Dorhout, D., Baas, M., Berné, S. & Sinninghe Damsté, J.S. (2014). Impact of river channel shifts on tetraether lipids in the Rhône prodelta (NW Mediterranean): Implication for the BIT index as an indicator of palaeoflood events. Organic Geochemistry, 75, 99-108

Published version: dx.doi.org/10.1016/j.orggeochem.2014.06.011

[Article begins on next page]

Impact of river channel shifts on tetraether lipids in the Rhône prodelta (NW Mediterranean): Implication for the BIT index as an indicator of palaeoflood events

Jung-Hyun Kim[a,*], Roselyne Buscail[b], Anne-Sophie Fanget[b,1], Frédérique Eyrolle-Boyer[c], Maria-Angela Bassetti[b], Denise Dorhout[a], Marianne Baas[a], Serge Berné[b,d], and Jaap S. Sinninghe Damsté[a]

[a] *NIOZ Royal Netherlands Institute for Sea Research, NL-1790 AB Den Burg, the Netherlands*

[b] *CEFREM-UMR CNRS 5110-University of Perpignan, 52 avenue Paul Alduy, F-66860, Perpignan, France*

[c] *Institut de Radioprotection et de Sûreté Nucléaire (IRSN), PRP-Env/SESURE/LERCM, BP3, Saint Paul Lez Durance, F-13115, France*

[d] *Ifremer, Géosciences Marines, BP 70, 29280 Plouzané, France*

[*]Corresponding author. Tel.: (+31) (0)222-369567.

E mail address: Jung-Hyun.Kim@nioz.nl (Jung-Hyun Kim).

[1]Present address: Centre for Past Climate Studies, Department of Geoscience, Aarhus University, Høegh-Guldbergs Gade 2, DK-8000 Aarhus C, Denmark

ABSTRACT

We tested the applicability of the BIT (branched and isoprenoid tetraether) index as a proxy for palaeoflood events in the river-dominated continental margin of the Gulf of Lions (NW Mediterranean). We compared the concentrations of branched glycerol dialkyl glycerol tetraethers (brGDGTs) and crenarchaeol in suspended particulate matter (SPM) collected downstream in the Rhône River, as well as in surface sediments and a ca. 8 m piston core retrieved from the Rhône prodelta. The core covered the last 400 yr, with four distinct intervals recording the river influence under natural and man-induced shifts in four main channels of the river mouth (Bras de Fer, Grand Rhône, Pégoulier, and Roustan). Our results indicate that there are mixed sources of brGDGTs and crenarchaeol in the Rhône prodelta, complicating application of the BIT index as an indicator of continental organic carbon input and, thus, as a palaeoflood proxy. However, the sedimentary BIT record for the period when continental material was delivered by the river more directly to the core site (Roustan phase; 1892 to present) mimics the historical palaeoflood record. This shows the potential of the BIT index as a palaeoflood proxy, provided that the delivery route of the continental material by rivers to the core sites remains constant over time. Our study also highlights the idea that shifts in river channels should be taken into account for the use of the BIT index as a palaeoflood proxy.

Keywords: palaeoflood, BIT index, GDGTs, Rhône prodelta

1. Introduction

The Earth's surface temperature rose by 0.6 ± 0.2°C over the 20th century, with accelerated warming during the past two decades (IPCC, 2013). With a warmer climate, the water-holding capacity of the atmosphere and evaporation to the atmosphere increase (e.g. Trenberth et al., 2003). Therefore, it would be expected that perturbations of the global water cycle would accompany global warming (e.g. Allen and Ingram, 2002). The possibility of increased precipitation intensity and variability is projected to boost the risks of extreme events such as typhoons/cyclones, droughts, and floods (IPCC, 2013). Many countries in temperate and tropical zones are highly vulnerable to such extreme events, exposing their coastal areas, including deltas, and their dense population to substantial human and economic consequences. Although the global climate models used for projections of future climate changes in the IPCC fifth assessment have been improved since the IPCC fourth assessment, the numerical model simulations still have difficulty in producing precipitation forecasts consistent with observations, whereas the prediction of temperature is more accurate (IPCC, 2013). Consequently, accurate predictions of changes in precipitation are more difficult to evaluate from current climate models. Therefore, the claim of increasing magnitude of extreme events due to global warming needs to be verified against paleodata with precise age dating, providing records of variation of precipitation that have actually occurred in the past.

Instrumental records of river flows have been used to establish statistical relationships between weather and runoff, which has been applied to predict hydrological changes in the future (e.g. Prudhomme et al., 2002). However, instrumental records of water discharge are too short to evaluate long term variation and already fall within the period of suggested strong human impact on natural conditions. The study of paleohydrological responses to past global climate changes can provide valuable information for indicating the potential impact of the present greenhouse global climate change and therefore contribute to design strategies for water and risk management (e.g. Gregory et al., 2006). Therefore, a wide range of tools and analytical techniques have been developed to extend hydrological data beyond the instrumental period of historical and geological scales: geological/geomorphological data (e.g. Starkel, 2003; Baker, 2006; Gregory et al., 2006), fossil pollen and plant macrofossil data (e.g. Bonnefille and Chalié, 2000), δD and $\delta^{13}C$ data for higher plant derived leaf wax (e.g. Schefuß et al., 2005) and a process-based vegetation model (Hatté and Guiot, 2005). Nonetheless, reconstruction of paleohydrological change is still challenging, with seemingly no consensus on the occurrence of reconstructed millennial-scale variation. Continuous palaeoflood records beyond the instrumental period are rare or too short to assess natural variation in flood occurrences related to climate change. Establishing a proxy which can be used for palaeoflood reconstruction is therefore desirable.

Due to the development of high pressure liquid chromatography-mass spectrometry (HPLC-MS) techniques for the analysis of glycerol dialkyl glycerol tetraethers (GDGTs) (Hopmans et al., 2000), the branched and isoprenoid tetraether (BIT) index was introduced as a tool, initially for estimating the relative amounts of river borne terrestrial organic carbon (OC) in marine sediments (Hopmans et al., 2004) and later more specifically as a proxy for river borne soil OC input (Huguet et al., 2007; Walsh et al., 2008; Kim et al., 2009; Smith et al. 2010). The index is based on a group of branched GDGTs (brGDGTs, Fig. 1), presumably derived from anaerobic bacteria (Weijers et al., 2006), which occur widely in soils (Weijers et al., 2007), and a structurally related isoprenoid GDGT, crenarchaeol (Fig. 1), predominantly produced by marine planktonic Group I Crenarchaeota (Sinninghe Damsté et al., 2002; see also Table 4 in Schouten et al., 2013), which was recently reclassified as the novel phylum Thaumarchaeota (Brochier-Armanet et al., 2008; Spang et al., 2010). The index has also shown potential as a proxy for paleohydrology change (Ménot et al., 2007; Verschuren et al., 2009). However, it has also been shown that variation in the index in marine sediments may predominantly reflect variation in marine crenarchaeol production rather than the soil-derived brGDGT flux (e.g. Weijers et al., 2009; Fietz et al., 2011; Smith et al., 2012). Therefore, it is necessary to further assess its applicability for paleostudies of diverse river systems by constraining the source of brGDGTs and crenarchaeol.

We previously performed several studies of the BIT index in the Têt River system (France), which has a relatively small catchment area, and in the Gulf of Lions (NW Mediterranean) into which the Têt River and Rhône River flow (Kim et al., 2006, 2007, 2009, 2010). A suspended particulate matter (SPM) study of the Têt River showed that variation in the concentration of brGDGTs was closely related to water and sediment discharges (Kim et al., 2007). The average BIT value for the Têt suspended particles (0.85) was substantially higher than that for the offshore seawater (< 0.01). Studies of marine surface sediments in the Gulf of Lions showed that the BIT index decreased from the inner shelf to the continental slope (Kim et al., 2006, 2010). Analysis of sediment trap and multicore material collected from the Têt inner shelf showed that the proportion of soil OC to total OC calculated on the basis of the BIT index was higher during flood periods than non-flood periods (Kim et al., 2009).

Although previous studies showed that the index was able to trace the input of soil OC in the Gulf of Lions, its applicability as a proxy for palaeoflood events was not assessed for the river-dominated continental margin of the Gulf of Lions. Therefore, we have extended our previous studies, by analysing the SPM from the downstream Rhône, as well as sediment samples from a 43 cm multicore and a ca. 8 m piston core from the Rhône prodelta. We compared GDGT data from the piston core with ostracod data from Fanget et al. (2013), which identified the extreme flood events based on the occurrence of freshwater (continental) ostracods. This enabled us to constrain the applicability of the BIT index as a palaeoflood indicator in the Gulf of Lions.

2. Study area

The Gulf of Lions is a river dominated continental margin in the NW Mediterranean Sea between 42°N 3°E and 44°N 6°E (Fig. 2). Freshwater and sediment inputs to the gulf originate mainly from the Rhône River, which has a catchment area of 97,800 km² and a length of 812 km, with its source in the Alps. The mean annual water discharge is ca. 1700 m^3/s and the annual solid discharge varies between 2 and 20 x 10^6 tonnes, with flood events responsible for > 70% of these amounts (Pont et al, 2002; Eyrolle et al, 2006, 2012; Sabatier et al., 2006). In the marine coastal area, close to the river mouth, both flocculation and aggregation lead to the formation of fine grained deposits, i.e. the subaqueous prodelta (30 km²). Most of the sediment delivered by the river is primarily entrapped in the prodelta (Ulses et al., 2008), characterized by a sediment accumulation rate of up to 20–50 cm/yr (Calmet and Fernandez, 1990; Charmasson et al., 1998; Radakovitch et al., 1999). Sedimentation rate strongly decreases seaward, with values of 0.2–0.6 cm/yr at 20 km distance (Miralles et al., 2005). The prodelta cannot, however, be considered as a permanent sedimentary repository since it is subject to episodic reworking (Marion et al., 2010) and subsequent seaward export through several turbid layers, i.e. nepheloid layers (Aloïsi et al., 1982; Estournel et al., 1997; Naudin and Cauwet, 1997).

3. Material and methods

3.1. Sample collection

The SPM samples are listed in Table 1 and sampling positions are shown in Fig. 2. Six SPM samples were collected close to the water surface and the bottom of the Rhône River at three different stations (RW1, RW2, and RW3). At the river mouth (RW4), the samples were collected at four different water depths. The hydrodynamics and mixing of river water with marine water in the estuary is typical of a micro-tidal salt wedge estuary (Ibañez et al., 1997). The salt marine water forms a wedge in the river water column underneath the freshwater layer. Therefore, we considered three SPM samples from beneath the surface layer at the river mouth as mixed SPM from both seawater and freshwater. For elemental analysis of SPM and the concentration, water was collected manually with a bucket. A small portion of the collected water (0.5-0.7 l) was filtered onto ashed (450 °C, overnight) and pre-weighed glass fibre filters (Whatman GF-F, 0.7 μm, 47 mm diam.). For lipid analysis 5-23 l water were filtered onto ashed glass fibre filters (Whatman GF-F, 0.7 μm, 142 mm diam.) with an in-situ pump system, (WTS, McLane Labs, Falmouth, MA). All samples were kept frozen at -20°C and freeze dried before analysis.

The multicore Dyneco 23B (Fig. 2) was retrieved from the Roustan prodeltaic lobe at 46 m water depth (43.307N; 4.855E) during the RHOSOS cruise (R/V Le Suroît) in September 2008. The surface sediment (0-0.5 cm) was sliced and immediately deep frozen on board. The piston core RHS-KS57 (Fig. 2) was obtained from 79 m water depth (43.285N; 4.8495E) during the same cruise. The age model of this core was established using radioactive ^{137}Cs, isotopic Pb ratio (^{206}Pb/^{207}Pb) and one accelerator mass spectrometer (AMS) ^{14}C date on a well-preserved *Turritella* sp. as described by Fanget et al. (2013). The core was subsampled at 5 cm intervals for elemental and GDGT analyses. The samples were freeze dried and homogenized prior to analysis.

3.2. Bulk geochemical analysis

The OC content of the marine sediments was obtained using an elemental analyser (LECO CN 2000 at CEFREM), after acidification with 2 M HCl (overnight, 50 °C) to remove carbonate. The OC data for core RHS-KS57 were published by Fanget et al. (2013). The freeze dried filter samples were decarbonated with HCl vapor as described by Lorrain et al.

(2003) and analysed with a Thermo Flash EA 1112 Elemental Analyzer. The OC content was expressed as wt. % dry sediment. The analyses were determined at least in duplicate. The analytical error was on average better than 0.2 wt. %.

3.3. Lipid extraction and purification

The filters on which SPM was collected (in total 10 samples) were freeze dried and extracted using a modified Bligh and Dyer method (White et al., 1979; Pitcher et al., 2009) in order to analyse core lipids and intact polar lipids. The Bligh and Dyer extracts (BDEs) were separated over a small silica gel (activated overnight) column with *n*-hexane:EtOA (1:1, v:v) and MeOH as eluents for core lipids and intact polar lipids, respectively. For GDGT quantification, 0.01 µg of C_{46} GDGT internal standard was added to each fraction. The core lipid fractions from the BDEs were separated into two fractions over an Al_2O_3 column (activated 2 h at 150 ˚C) using hexane:DCM (1:1, v:v) and DCM:MeOH (1:1, v:v), respectively.

For the upper 3 m of core RHS-KS57, GDGTs were analysed every ca. 5 cm, and every ca. 10 cm between 3 m and 7.7 m (in total 79 samples). These core samples and the core top sediment of multicore Dyneco 23B were extracted with an accelerated solvent extractor (DIONEX ASE 200) using DCM:MeOH (9:1, v:v) at 100 °C and 1500 psi. The extracts were collected in vials. Solvents were removed using Caliper Turbovab®LV, and the extracts were taken up in DCM, dried over anhydrous Na_2SO_4, and blown down under a stream of N_2. For quantification of GDGTs, 0.1 µg internal standard (C_{46} GDGT) was added to each total extract before it was separated into three fractions over an activated Al_2O_3 column using hexane:DCM (9:1, v:v), hexane:DCM (1:1, v:v) and DCM:MeOH (1:1, v:v).

3.4. GDGT analysis and BIT calculation

For the SPM samples, the analysis of GDGTs in core and intact polar lipid fractions was carried out as described by Zell et al. (2013a). For the marine sediments, the polar DCM:MeOH fractions were analyzed for core lipid GDGTs as described by Schouten et al. (2007). The fractions were dried down under N_2, redissolved by sonication (5 min) in *n*-hexane:propan-2-ol (99:1, v:v) to a concentration of ca. 2 mg/ml and filtered through 0.45 µm PTFE filters. The samples were analyzed using HPLC-APCI-MS according to the procedure described by Schouten et al. (2007), with minor modifications. GDGTs were detected using selective ion monitoring of $(M+H)^+$ ions (dwell time 237 ms) and quantification was achieved by integrating peak areas and using the C_{46} GDGT internal standard according to Huguet et al. (2006). Note that the two different extraction methods used for quantification of GDGTs of core lipids would provide comparable results (cf. Lengger et al., 2012).

The BIT index was calculated according to Hopmans et al. (2004):

$$\text{BIT index} = \frac{[\text{I}]+[\text{II}]+[\text{III}]}{[\text{I}]+[\text{II}]+[\text{III}]+[\text{IV}]} \quad (1)$$

The roman numerals refer to the GDGTs indicated in Fig. 1. I, II and III are brGDGTs and IV is crenarchaeol (Hopmans et al., 2004). The reproducibility in the determination of the BIT index was better than ±0.01. The BIT index varies between 0 and 1, representing marine and terrestrial OC end members, respectively (Hopmans et al., 2004).

3.5. Statistical analysis

We performed the nonparametric Mann-Whitney U test, which does not meet the normality assumption of the one way analysis variance (ANOVA), to evaluate the differences in mean values between two different groups in a similar way to Zell et al. (2013). Groups that showed significant difference ($p < 0.05$) were assigned different letters. Linear regression analysis was also performed to investigate the relationship between GDGT parameters. The statistical tests were performed using the R-3.0.1 package.

4. Results

The SPM concentration and OC content of Rhône River SPM samples are summarized in Table 1. SPM concentration varied between 12 and 15 mg/L and the OC content of the SPM was relatively constant at 2-3 wt. %. BrGDGTs and crenarchaeol were detected in all the SPM samples. Summed brGDGT concentration (normalized to OC content) ranged from 8 to 36 μg/g OC (av. 16 ± 9, $n=7$; Fig. 3A), while crenarchaeol concentration was substantially lower, i.e. between 1 and 4 μg/g OC (av. 2 ± 1, $n=7$; Fig. 3B). The BIT index averaged 0.89 ± 0.02 ($n=7$; Fig. 3C). Summed brGDGT concentration values for the SPM samples from the mixed zone, i.e. beneath the surface layer at the river mouth as a mixture of both seawater and freshwater, were slightly lower than those in the river, with an average value of 11 ± 3 μg/g OC ($n=3$; Fig. 3A). In contrast, the crenarchaeol concentration was higher, ranging from 4 to 7 μg/g OC (av. 6 ± 1 μg/g OC, $n=3$; Fig. 3B). Consequently, the BIT index was lower, varying between 0.56 and 0.81 (av. 0.65 ± 0.11, $n=3$; Fig. 3C).

BrGDGTs and crenarchaeol were also detected in all marine sediment core samples. The concentrations of summed brGDGTs and crenarchaeol as well as the BIT index for the core top sediment from the Dyneco 23B multicore were 8 μg/g OC and 5 μg/g OC, and 0.64, respectively (Fig. 3; data points indicated with a star). The summed brGDGT concentration of for piston core RHS-KS57 varied between 2 and 14 μg/g OC, while the concentration of crenarchaeol ranged from 3 to 45 μg/g OC (Fig. 4A-B). The records of the accumulation rate (AR) of these GDGTs mimicked those of their concentration, varying between 0.02 and 0.38

(μg/cm^2/yr) for summed brGDGTs and between 0.02 and 0.82 (μg/cm^2/yr) for crenarchaeol, respectively (Fig. 4). The BIT index varied widely between 0.17 and 0.78 (Fig. 4C).

5. Discussion

5.1. Present-day source of GDGTs in the Rhône River and prodelta system: consequences for the BIT index

Our SPM results only provide "snap-shot" information at the time of sampling and should thus be interpreted cautiously. The BIT index for the riverine SPM revealed only a narrow range of variation (0.89 ± 0.02, *n=7*; Fig. 3). The riverine BIT values were slightly lower than the hypothetical terrestrial end member value of 1 (Hopmans et al., 2004). This is most probably due to the production of crenarchaeol in soil as shown in the drainage basin of the Têt River, a typical small Mediterranean river, which flows into the Gulf of Lions, with an average BIT value of 0.84 (Kim et al., 2010). SPM of the Têt River also has locally lower BIT values (down to 0.6), which has been explained by crenarchaeol production in the river (Kim et al., 2007). In situ production of crenarchaeol in other rivers has also been reported (e.g. Zell et al., 2013a,b; Yang et al., 2013). It is also possible that brGDGTs were produced in the Rhône River itself, as reported for other river systems (Zhu et al., 2011; Kim et al., 2012; Zhang et al., 2012; Yang et al., 2013; Zell et al., 2013a,b; De Jonge et al., 2014). Hence, GDGTs in Rhône River SPM might have a mixed source of soil- and river-produced brGDGTs and crenarchaeol. Nevertheless, despite potential in situ production, BIT values were high in the river itself, consistent with the original proposition for the BIT index (Hopmans et al., 2004).

Values of the BIT index of SPM in the mixed zone significantly decreased in comparison with that of riverine SPM (Fig. 3C). This is caused by the substantial increase in crenarchaeol concentration in the mixed zone of seawater and freshwater at the Rhône River mouth (Fig. 3B), while that of the brGDGTs remained comparable (Fig. 3A). The index decreased further in the prodelta sediments (Fig. 3C). This suggests that there is in fact an addition of crenarchaeol, most likely by in situ production in the water column by Thaumarchaeota but we cannot completely exclude a potential benthic production (cf. Lengger et al., 2012). Recent studies provide increasing evidence that brGDGTs can also be produced in coastal sediments (Peterse et al., 2009; Zhu et al., 2011). However, similar brGDGT concentrations (normalized on OC) were found in the Rhône River SPM and the mixed zone SPM compared with that of the Rhône prodelta surface sediment (indicated with a star in Fig. 3). This suggests that the in situ production of brGDGTs in the marine sediments might have no significant impact on the BIT index, as also observed for Svalbard fjord sediments (Peterse et al., 2009) and the East China Sea (Zhu et al., 2011). Our observation leads us to conclude that, in the present day system, brGDGTs are primarily transported from the Rhône watershed to the Rhône prodelta but the BIT index in prodelta sediments is strongly influenced by enhanced contribution of crenarchaeol produced by nitrifying Thaumarchaeota (Könneke et al., 2005; Wuchter et al., 2006) thriving in the marine environment.

5.2. Applicability of BIT index as an indicator of palaeoflood events

In a study of the BIT index in the Têt River system (France), Kim et al. (2007) showed that the variation in concentration of riverine brGDGTs was closely related to water and sediment discharges from the river, with substantially higher BIT value (0.85) than that for the offshore seawater (< 0.01) in the Gulf of Lions. Furthermore, brGDGT concentration and the BIT index in sediment trap and multicore material were much higher during the flood period than during non-flood periods in the Têt prodelta (Kim et al., 2009). In the Rhône prodelta, brGDGT concentration and the BIT index were much higher than at offshore sites

(Kim et al., 2010). This promoted the idea that BIT index, in conjunction with brGDGT concentration, might serve as a tool for reconstructing palaeoflood events in deltaic systems of the Gulf of Lions. To assess this possibility, we further investigated the evolution of brGDGT and crenarchaeol concentrations in the Rhône prodelta during the last 400 yr and evaluated the consequences for the BIT index, by analysing the 7.71 m RHS-KS57 piston core obtained in 79 m deep water (Fig. 2).

Fanget et al. (2013) reconstructed paleoenvironmental changes based on ostracod and benthic foraminiferal assemblages recorded in the core. They identified four intervals recording changes in river influence under natural and man-induced shifts in Rhône distributaries and corresponding to deltaic lobes: Bras de Fer, Grand Rhône, Pégoulier, and Roustan (Fig. 4). The Bras de Fer interval (771-590 cm, up to 1711 AD) is characterized by quite stable environmental conditions, low hydrodynamic energy and dominant marine benthic microfossil species. The south-westward direction of the Rhône plume (Estournel et al., 1997, Naudin and Cauwet, 1997) probably caused reduced river influence at the core site at that time. During the “Grand Rhône” interval (590-360 cm, 1711-1855 AD), ostracod assemblages are dominated by the shallow water species *Loxoconcha* spp. which are found in marginal marine environments (delta and estuarine) characterized by changing salinity and sediment flux. Following an important flood in 1711 AD, the Bras de Fer channel shifted towards the east and thus was similar to the present day position of the Grand Rhône River. Between 1711 AD and 1852 AD, the seaward termination of the Grand Rhône River was divided into three distributaries called Piémanson, Roustan, and Pégoulier channels (Fig. 2). By that time, the Rhône River mouth was located upstream Port Saint Louis, i.e. > 6 km inland from the modern position, resulting in a moderate river influence at the core site. The “Pégoulier” interval (360-280 cm, 1855-1892 AD) is highly comparable to the Bras de Fer interval in terms of micro-faunal content. It corresponds to the period of artificial closure of the Piémanson and Roustan channels in 1855 AD. Consequently, the water and sediment discharges were funnelled into a single mouth, the Pégoulier channel, located at the eastern most part of the modern delta. Sediment flux was thus focused to the east of the prodelta to contribute to the building of the Pégoulier outlet. The “Roustan” interval (0-280 cm, 1892 AD to present) shows a strong decrease of marine ostracods and a concomitant increase in the deltaic assemblage (Fig. 4D-E). In addition, freshwater ostracods (i.e. *Candona* sp., *Ilyocypris* sp.) appear at discrete levels, generally in correlation with ostracods typical of the littoral areas (i.e. *Leptocythere* sp., *Pterigocythereis* sp.). Ostracod fauna indicate a significant increase in the Rhône River influence at the core site. According to our age model, the gradual increase in the river influence indicates a more proximal source and reflects the present situation, with the Rhône River flowing into the Gulf of Lions through the Roustan channel since 1892 AD, where our core was located (Fig. 2).

In general, the summed brGDGT concentration and the BIT index were significantly lower in the sediments than in the river SPM, while the crenarchaeol concentration was much higher (Fig. 3). For the entire piston core dataset, crenarchaeol concentration and accumulation rate significantly correlated with (Fig. 5A) those of the summed brGDGTs (R^2 0.29, $p < 0.001$, and R^2 0.59, $p < 0.001$, respectively). Positive correlations between the concentrations of crenarchaeol and brGDGTs have been reported for various marine settings (e.g. Yamamoto et al., 2008; Zhu et al., 2011; Fietz et al., 2012) but not for accumulation rates. With respect to the four separate sedimentary phases, significant positive correlations between crenarchaeol and brGDGTs for both the concentrations and the accumulation rates occurred only during Grand Rhône (1711-1855 AD) and Roustan (1892 AD-present) phases (Table 2), when the Grand Rhône and Roustan channels were located right at the front of the core site (Fig. 2). During these periods, the crenarchaeol concentration was similar to that of SPM in the mixing zone (Fig. 3). Various studies have found that marine Thaumarchaeota are nitrifiers and their abundance is dependent on primary productivity since organic N is converted upon decay of algal biomass to NH_4^+ (e.g. Wuchter et al., 2006; Sinninghe Damsté et al., 2009). Hence, enhanced riverine nutrient delivery to the continental margins may stimulate primary productivity and thus, indirectly, increase Thaumarchaeotal abundance and crenarchaeol production, resulting in a decrease in the BIT index. This probably explains the co-variation of brGDGT and crenarchaeol concentrations, as well as of brGDGT and crenarchaeol accumulation rates in our records (Fig. 5A).

During all phases (Table 2), the (negative) correlations for both concentration and accumulation rate of crenarchaeol with the BIT index (Fig. 5B) were much stronger and more significant than the (positive) correlations of brGDGT concentration and accumulation rate with the BIT index (Fig. 5C). The correlation between crenarchaeol and the BIT index was highest during the Bras de Fer phase (reflected by the lower section of the core; 771-590 cm, up to 1711 AD), when the Rhône River flowed into the Gulf of Lions through the Bras de Fer channel (which is located more to the west; Fig. 2) and thus the river influence was lowest at the core site (Fig. 5; Table 2). The variation in crenarchaeol concentration (3-45 μg/g OC) was substantially greater than that in brGDGT abundance (2–14 μg/g OC) (Fig. 4). Remarkably, despite the overall low brGDGT accumulation rates (<0.1 μg/cm^2/yr), only during this Bras de Fer phase the correlation between the brGDGT accumulation rate and the BIT index was significant (Table 2). Nevertheless, it appears that during this phase the BIT index was more strongly governed by crenarchaeol production in the marine environment than by the input of brGDGTs from the Rhône River. Accordingly, these results support the proposition that the riverine brGDGTs are not always the first order factor controlling the BIT index in marine sediments but the variation in marine-derived crenarchaeol abundance is (cf. Castañeda et al., 2010; Fietz et al., 2011a,b, 2012; Wu et al., 2013). However, it does not explain why BIT values are higher along the coast than those offshore in the Gulf of Lions

(Kim et al., 2010), as well as in the vicinity of large rivers (e.g. Hopmans et al., 2004). In certain locations, brGDGTs transported from the rivers might more strongly influence the BIT index than marine-derived crenarchaeol, although we cannot rule out an additional contribution of brGDGTs from the coastal erosion.

Importantly, we also observed that variations in crenarchaeol and thus in BIT index were strongly influenced by Rhône River channel shifts. During the “Grand Rhône” and “Roustan” river-dominated phases, the BIT index was more strongly governed by variation in riverine brGDGTs than during “Bras de Fer” and “Pégoulier” marine-dominated phases. When the Rhône River mouth was located right at the front of the core site during the Roustan phase (Fig. 2), the accumulation rates of both brGDGTs and crenarchaeol were much higher than during other phases (Fig. 4). Interestingly, during the Roustan phase, the BIT index was well in phase, within the age uncertainty, with the historical palaeoflood record (> 4.0 m at Arles; i.e. when the river level was > 5.25 m above mean sea level; Pichard, 1995; Fig. 6). As proposed for the Yellow River-dominated Bohai Sea (Wu et al., 2013), highly turbid river flow might play a key role in the BIT index when the river mouth has shifted closer to the core site. Highly turbid river flow carries more SPM to the marine sites and thus reduces water transparency, providing unfavourable conditions for primary production (Turner et al., 1990). As a result, fewer Thaumarchaeota might be produced and thus less crenarchaeol might accumulate in marine sediments, whilst the input of riverine brGDGTs increases, amplifying the magnitude of the BIT index.

6. Conclusions

Our study indicates that brGDGTs were transported primarily from the Rhône watershed to the Rhône prodelta and that the contribution of marine produced brGDGTs was minor. However, the BIT index showed a stronger correlation with crenarchaeol concentration than with brGDGT concentration, indicating that the BIT index in Rhône prodelta sediments was primarily influenced by variation in marine crenarchaeol production rather than by the delivery of riverine brGDGTs. This complicates the application of the BIT index as an indicator for the input of continental OC and thus as a palaeoflood proxy. Furthermore, it was observed that the shifts in the Rhône distributaries controlled the distribution of allochthonous and autochthonous brGDGTs and crenarchaeol at the core site. When the continental material was delivered by the Rhône River more directly to the core site (Roustan phase), the BIT index strongly mimicked the historical palaeoflood record. This shows the potential of the BIT index for tracing palaeoflood events and thus for providing palaeoflood records on longer geological time-scales beyond the instrumental period, assuming that no major change affected the course of the river channel. Our study also highlights the idea that variation in the delivery route of continental OC by rivers to core sites should be taken into account for the use of the BIT index as a palaeoflood proxy.

Acknowledgments

We thank Dr. R. W. Smith and an anonymous reviewer for their constructive comments. We also thank to J. Ossebaar and E. Hopmans at NIOZ for their analytical support and the crew of the R/V Le Suroît and the science party of the "RHOSOS" cruise for retrieving the cores. The research leading to these results has received funding from the European Research Council under the European Union's Seventh Framework Programme (FP7/2007-2013) / ERC grant agreement n° [226600]. The work was also supported by the CHACCRA (Climate and Human induced Alterations in Carbon Cycling at the River-seA connection) and EXTREMA (Impact of extreme events on the transfer of anthropogenic pollutants in the coastal zone continuum of the Gulf of Lion - NW Mediterranean Sea) projects funded by the French

National Research Agency. Additional support was provided to A.S.F. through the Mistrals/Paleomex Programme of INSU/CNRS (France).

References

Allen, M.R., Ingram, W.J., 2002. Constraints on future changes in climate and the hydrologic cycle. Nature 419, 224–232.

Aloïsi, J.C., Cambon, J.P., Carbonne, J., Cauwet, G., Millot, C., Monaco, A., Pauc, H., 1982. Origine et rôle du néphéloïde profond dans le transfert des particules au milieu marin. Application au Golfe du Lion. Oceanologica Acta 5, 481–491.

Bligh, E.G., Dyer, W.J., 1959. A rapid method of total lipid extraction and purification. Canadian Journal of Biochemistry and Physiology 37, 911–917.

Bonnefille, R., Chalié, F., 2000. Pnolle-inferred precipitation time -series from Equatorial mountains, Africa, the last 40 kyr BP. Global and Planetary Change 26, 25–50.

Brochier-Armanet, C., Boussau, B., Gribaldo, S., Forterre, P., 2008. Mesophilic crenarchaeota: proposal for a third archaeal phylum, the Thaumarchaeota. Nature Reviews Microbiology 6, 245–252.

Calmet, D., Fernandez, J.-M., 1990. Caesium distribution in northwest Mediterranean seawater, suspended particles and sediments. Continental Shelf Research 10, 895–913.

Castañeda, I.S., Schefuß, E., Pätzold, J., Sinninghe Damsté, J.S., Weldeab, S., Schouten, S., 2010. Millennial-scale sea surface temperature changes in the eastern Mediterranean (Nile River Delta region) over the last 27,000 years. Paleoceanography 25, doi: 10.1029/2009PA001740.

Charmasson, S., Radakovitch, O., Arnaud, M., Bouisset, P., Pruchon, A., 1998. Long-cores profiles of ^{137}Cs, ^{134}Cs, ^{60}Co and ^{210}Pb in sediment near the Rhône River (Northwestern Mediterranean Sea). Estuaries 21, 367–378.

Estournel, C., Kondrachoff, V., Marsaleix, P., Vehil, R., 1997. The plume of the Rhone: numerical simulation and remote sensing. Continental Shelf Research 17, 899–924.

Eyrolle, F., Duffa, C., Antonelli, C., Rolland, B., Leprieur, F., 2006. Radiological consequences of the extreme flooding on the lower course of the Rhone valley (December 2003, South East France). Science of the Total Environment 366, 427–438.

Eyrolle, F., Radakovitch, O., Raimbault, P., Charmasson, S., Antonelli, C., Ferrand, E., Aubert, D., Raccasi, G., Jacquet, S., Gurriaran, R. 2012. Consequences of hydrological events on the delivery of suspended sediment and associated radionuclides from the Rhône River to the Mediterranean Sea. Journals of Soils and Sediments, doi:10.1007/s11368-012-0575-0.

Fanget, A.-S., Bassetti, M.-A., Arnaud, M., Chiffoleau, J.-F., Cossa, D., Goineau, A., Fontanier, C., Buscail, R., Jouet, G., Maillet, G.M., Negri, A., Dennielou, B., Berné, S., 2013. Historical evolution and extreme climate events during the last 400 years on the Rhone prodelta (NW Mediterranean). Marine Geology, 346, 375-391.

Fietz, S., Martínez-Garcia, A., Huguet, C., Rueda, G., Rosell-Melé, A., 2011a. Constraints in the application of the Branched and Isoprenoid Tetraether index as a terrestrial input proxy. Journal of Geophysical Research: Oceans 116, C10032. http://dx.doi.org/10.1029/2011JC007062.

Fietz, S., Martínez-Garcia, A., Rueda, G., Peck, V.L., Huguet, C., Escala, M., Rosell-Melé, A., 2011b. Crenarchaea and phytoplankton coupling in sedimentary archives: common trigger or metabolic dependence? Limnology and Oceanography 56, 1907–1916.

Fietz, S., Huguet, C., Bendle, J., Escala, M., Gallacher, C., Herfort, L., Jamieson, R., Martínez-Garcia, A., McClymont, E.L., Peck, V.L., Prahl, F.G., Rossi, S., Rueda, G., Sanson-Barrera, A., Rosell-Melé, A., 2012. Co-variation of crenarchaeol and branched

GDGTs in globally-distributed marine and freshwater sedimentary archives. Global and Planetary Change 92–93, 275–285.

Gregory, K.J., Benito, G., Dikau, R., Golosov, V., Johnstone, E.C., Jones, J.A.A., Macklin, M.G., Parsons, A.J., Passmore, D.G., Poesen, J., Soja, R., Starkel, L., Thorndycraft, V.R., Walling, D.E., 2006. Past hydrological events and global change. Hydrological Processes 20, 199–204.

Hatté, C., Guiot J., 2005. Paleoprecipitation reconstruction by inverse modelling using the isotopic signal of loess organic matter: application to the Nußloch loess sequence (Rhine Valley, Germany). Climate Dynamics 25, 315–327.

Hopmans, E.C., Schouten, S., Pancost, R.D., van der Meer, M.T.J., Sinninghe Damsté, J.S., 2000. Analysis of intact tetraether lipids in archaeal cell material and sediments by high performance liquid chromatography/atmospheric pressure chemical ionization mass spectrometry. Rapid Communications in Mass Spectrometry14, 585–589.

Hopmans, E.C., Weijers, J.W.H., Schefuß, E., Herfort, L., Sinninghe Damsté, J.S., Schouten, S., 2004. A novel proxy for terrestrial organic matter in sediments based on branched and isoprenoidtetraether lipids. Earth and Planetary Science Letters 224, 107–116.

Huguet, C., Hopmans, E.C., Febo-Ayala, W., Thompson, D.H., Sinninghe Damsté, J.S., Schouten, S., 2006. An improved method to determine the absolute abundance of glycerol dibiphytanyl glycerol tetraether lipids. Organic Geochemistry 37, 1036–1041.

Huguet, C., Smittenberg, R.H., Boer, W., Sinninghe Damsté, J.S., Schouten, S., 2007. Twentieth century proxy records of temperature and soil organic matter input in the Drammensfjord, southern Norway. Organic Geochemistry 38, 1838–1849.

Ibañez, C., Pont, D., Prat, N., 1997. Characterization of the Ebre and Rhone estuaries: A basis for defining and classifying salt-wedge estuaries. Limnology and Oceanography 42, 89–101.

IPCC, 2013. Climate Change 2013: The Physical Science Basis. www.climatechange2013.org.

Kim, J.-H., Schouten, S., Buscail, R., Ludwig, W., Bonnin, J., Sinninghe Damsté, J.S., Bourrin, F., 2006. Origin and distribution of terrestrial organic matter in the NW Mediterranean (Gulf of Lions): Exploring the newly developed BIT index. Geochemistry Geophysics Geosystems 7, 1–20.

Kim, J.-H., Ludwig, W., Schouten, S., Kerherve, P., Herfort, L., Bonnin, J., Sinninghe Damsté, J.S., 2007. Impact of flood events on the transport of terrestrial organic matter to the ocean: A study of the Têt River (SW France) using the BIT index. Organic Geochemistry 38, 1593–1606.

Kim, J.-H., Buscail, R., Bourrin, F., Palanques, A., Sinninghe Damsté, J.S., Bonnin, J., Schouten, S., 2009. Transport and depositional process of soil organic matter during wet and dry storms on the Têt inner shelf (NW Mediterranean). Palaeogeography, Palaeoclimatology, Palaeoecology 273, 228–238.

Kim, J.-H., Zarzycka, B., Buscail, R., Peters, F., Bonnin, J., Ludwig, W., Schouten, S., Sinninghe Damsté, J.S., 2010. Contribution of river-borne soil organic carbon to the Gulf of Lions (NW Mediterranean). Limnology and Oceanography 55, 507–518.

Kim, J.-H., Zell, C., Moreira-Turcq, P., Pérez, M.A.P., Abril, G., Mortillaro, J.-M., Weijers, J.W.H., Meziane, T., Sinninghe Damsté, J.S., 2012. Tracing soil organic carbon in the lower Amazon River and its tributaries using GDGT distributions and bulk organic matter properties. Geochimica et Cosmochimica Acta 90, 163–180.

Kim, J.-H., Buscail, R., Fanget, A.-S., Eyrolle-Boyer, F., Bassetti, M.-A., Dorhout, D., Baas, M., Berné, S., and Sinninghe Damsté, J.S., 2014. Impact of river channel shifts on tetraether lipids in the Rhône prodelta (NW Mediterranean): Implication for the BIT index as an indicator of palaeoflood events. Organic Geochemistry, submitted.

Lengger, S.K., Hopmans, E.C., Sinninghe Damsté, J.S., Schouten, S., 2012. Comparison of extraction and work up techniques for analysis of core and intact polar tetraether lipids from sedimentary environments. Organic Geochemistry 47, 34–40.

Lorrain, A., Savoye, N., Chauvaud, L., Paulet, Y.-M., Naulet, N., 2003. Decarbonation and preservation method for the analysis of organic C and N contents and stable isotope ratios of low-carbonated suspended particulate material. Analytica Chimica Acta 491, 125–133.

Marion, C., Dufoisb, F., Arnaudb, M., Vellad, C., 2010. In situ record of sedimentary processes near the Rhône River mouth during winter events (Gulf of Lions, Mediterranean Sea). Continental Shelf Research 30, 1095–1107.

Ménot, G., Bard, E., Rostek, F., Weijers, J.W.H., Hopmans, E.C., Schouten, S., Sinninghe Damsté, J.S., 2006. Early reactivation of European rivers during the last deglaciation. Science 313, 1623–1625.

Miralles, J., Radakovitch, O., Aloïsi, J.C., 2005. ^{210}Pb sedimentation rates from the Northwestern Mediterranean margin. Marine Geology 216, 155–167.

Naudin, J.J., Cauwet, G., 1997. Transfer mechanisms and biogeochemical implications in the bottom nepheloid layer: A case study of the coastal zone off the Rhone River (France). Deep Sea Research Part II: Topical Studies in Oceanography 44, 551–575.

Peterse, F., Kim, J.-H., Schouten, S., Kristensen, D.K., Koç, N., Sinninghe Damsté, J.S., 2009. Constraints on the application of the MBT/CBT palaeothermometer at high latitude environments (Svalbard, Norway). Organic Geochemistry 40, 692–699.

Pichard, G., 1995. Les crues sur le bas-Rhône de 1500 à nos jours. Pour une histoire hydroclimatique. Méditerranée 3–4, 105–116.

Pitcher, A., Hopmans, E.C., Schouten, S., Sinninghe Damsté, J.S., 2009. Separation of core and intact polar archaeal tetraether lipids using silica columns: Insights into living and fossil biomass contributions. Organic Geochemistry 40, 12–19.

Pont, D., Simonnet, J.P., Walter, A.V, 2002. Medium-terms changes in suspended sediment delivery to the ocean: consequences of catchment heterogeneity and river management (Rhone River, France). Estuarine, Coastal and Shelf Science 54, 1–18.

Prudhomme, C., Reynard, N., Crooks, S., 2002. Downscaling of GCMs for flood frequency analysis: where are we now? Hydrological Processes 16, 1137–1150.

Radakovitch, O., Charmasson, S., Arnaud, M., Bouisset, P., 1999. ^{210}Pb and caesium accumulation in the Rhône delta sediments. Estuarine, Coastal and Shelf Science 48, 77–92.

Sabatier, P., Maillet, G., Provansal, M., Fleury, T.J., Suanez, S., Vella, C., 2006. Sediment budget of the Rhône delta shoreface since the middle of the 19th century. Marine Geology 234, 143–157.

Schefuß, E., Schouten, S., Schneider, R.R., 2005. Climatic controls on central African hydrology during the past 20,000 years. Nature, 437, 1003–1006.

Schmidt, F., Hinrichs, K.-U., Elvert, M., 2010. Sources, transport, and partitioning of organic matter at a highly dynamic continental margin. Marine Chemistry 118, 37–55.

Schouten, S., Huguet, C., Hopmans, E.C., Kienhuis, M., Sinninghe Damsté, J.S., 2007. Analytical methodology for TEX_{86} paleothermometry by High-Performance Liquid Chromatography/Atmospheric Pressure Chemical Ionization-Mass Spectrometry. Analytical Chemistry 79, 2940–2944.

Schouten, S., Hopmans, E.C., Sinninghe Damsté, J.S., 2013. The organic geochemistry of glycerol dialkyl glycerol tetraether lipids: A review. Organic Geochemistry 54, 19–61.

Smith, R.W., Bianchi, T.S., Savage, C., 2010. Comparison of lignin phenols and branched/isoprenoid tetraethers (BIT index) as indices of terrestrial organic matter in Doubtful Sound, Fiordland, New Zealand. Organic Geochemistry 41, 281–290.

Smith, R.W., Bianchi, T.S. and Li, X., 2012. A re-evaluation of the use of branched GDGTs as terrestrial biomarkers: Implications for the BIT Index. Geochimica et Cosmochimica Acta 80, 14–29.

Spang, A., Hatzenpichler, R., Brochier-Armanet, C., Rattei, T., Tischler, P., Spieck, E., Streit W., Stahl D.A., Wagner M., Schleper, C., 2010. Distinct gene set in two different lineages of ammonia-oxidizing archaea supports the phylum Thaumarchaeota. Trends in Microbiology 18, 331–340.

Trenberth, K.E., Dai, A.G., Rasmussen, R.M., Parsons, D.B., 2003. The changing character of precipitation. Bulletin of the American Meteorological Society 84, 1205–1217.

Turner, R.E., Rabalais, N.N., Nan, Z.Z., 1990. Phytoplankton biomass production and growth limitations on the Huanghe (Yellow River) continental shelf. Continental Shelf Research 10, 545–571.

Ulses, C., Estournel, C., Durrieu de Madron, X., Palanques, A., 2008. Suspended sediment transport in the Gulf of Lions (NW Mediterranean): impact of extreme storms and floods. Continental Shelf Research 28, 2048–2070.

Verschuren, D., Sinninghe Damsté, J.S., Moernaut, J., Kristen, I., Blaauw, M., Fagot, M., Haug, G.H., CHALLACEA project members, 2009. Half-precessional dynamics of monsoon rainfall near the East African Equator. Nature 462, 637–641.

Walsh, E.M., Ingalls, A.E., Keil, R.G., 2008. Sources and transport of terrestrial organic matter in Vancouver Island fjords and the Vancouver-Washington Margin: A multiproxy approach using $\delta^{13}C_{org}$, lignin phenols, and the ether lipid BIT index. Limnology and Oceanography 53, 1054–1063.

Weijers, J.W.H., Schouten, S., Hopmans, E.C., Geenevasen, J.A.J., David, O.R.P., Coleman, J.M., Pancost, R.D., Sinninghe Damsté, J.S., 2006. Membrane lipids of mesophilic anaerobic bacteria thriving in peats have typical archaeal traits. Environmental Microbiology 8, 648–657.

Weijers, J.W.H., Schouten, S., van den Donker, J.C., Hopmans, E.C., Sinninghe Damsté, J.S., 2007. Environmental controls on bacterial tetraether membrane lipid distribution in soils. Geochimica et Cosmochimica Acta 71, 703–713.

Weijers, J.W.H., Schouten, S., Schefuss, E., Schneider, R.R., Sinninghe Damsté, J.S., 2009. Disentangling marine, soil and plant organic carbon contributions to continental margin sediments: A multi-proxy approach in a 20,000 year sediment record from the Congo deep-sea fan. Geochimica et Cosmochimica Acta 73, 119–132.

White, D.C., Davis, W.M., Nickels, J.S., King, J.D., Bobbie, R.J., 1979. Determination of the sedimentary microbial biomass by extractable lipid phosphate. Oecologia 40, 51–62.

Wu, W., Zhao, L., Pei, Y., Ding, W., Yang, H., and Xu, Y., 2013. Variability of tetraether lipids in Yellow River-dominated continental margin during the past eight decades: Implications for organic matter sources and river channel shifts. Organic Geochemistry 60, 33–39.

Yang, G., Zhang, C.L., Xie, S., Chen, Z., Gao, M., Ge, Z., Yang, Z., 2013. Microbial glycerol dialkyl glycerol tetraethers from river water and soil near the Three Gorges Dam on the Yangtze River. Organic Geochemistry 56, 40–50.

Zell, C., Kim, J.-H., Moreira-Turcq, P., Abril, G., Hopmans, E.C., Bonnet, M.-P., Lima Sobrinho, R., Sinninghe Damsté, J.S., 2013a. Disentangling the origins of branched tetraether lipids and crenarchaeol in the lower Amazon River: Implications for GDGT-based proxies. Limnology and Oceanography 58, 343–353.

Zell, C., Kim, J.-H., Abril, G., Sobrinho, R.L., Dorhout, D., Moreira-Turcq, P., Sinninghe Damsté, J.S., 2013b. Impact of seasonal hydrological variation on the distributions of tetraether lipids along the Amazon River in the central Amazon basin: Implications for the MBT/CBT paleothermometer and the BIT index. Frontiers in Microbiology 4, doi: 10.3389/fmicb.2013.00228, 2013.

Zhang, C.L., Wang, J., Wei, Y., Zhu, C., Huang, L., Dong, H., 2012. Production of branched tetraether lipids in the lower Pearl River and estuary: effects of extraction methods and impact on bGDGT proxies. Frontiers in Microbiology 2, doi: 10.3389/fmicb.2011.00274.

Zhu, C., Weijers, J.W.H., Wagner, T., Pan, J.M., Chen, J.F., Pancost, R.D., 2011. Sources and distributions of tetraether lipids in surface sediments across a large river-dominated continental margin. Organic Geochemistry 42, 376–386.

Figure captions

Fig. 1. Structure of brGDGTs (I-III) and crenarchaeol (IV).

Fig. 2. Map showing the sampling locations of SPM along the Rhône River (RW1, RW2, RW3, and RW4) and multicore Dyneco 23B and piston core RHS-KS57 from the Rhône prodelta (NW Mediterranean).

Fig. 3. Box plot of A) summed brGDGTs (μg/g OC), B) crenarchaeol (μg/g OC), and C) BIT index from SPM collected in October 2010 and piston core RHS-KS57 collected in September 2008. Core top sediment data from multicore Dyneco 23B are indicated with a red star. Letters indicate statistically significant groups of data ($p < 0.05$).

Fig. 4. Vertical profile of A) summed brGDGTs for concentration (μg/g OC, black line) and accumulation rate ($\mu g/cm^2/yr$, red line), B) crenarchaeol for concentration (μg/g OC, black line) and accumulation rate ($\mu g/cm^2/yr$, red line), C) BIT index, D) ostracod fresh water assemblage (%), and E) ostracod full marine assemblage (%) from piston core RHS-KS57. Ostracod data are from Fanget et al. (2013). Filled triangles indicate age control points.

Fig. 5. Cross plots A) between crenarchaeol and summed brGDGTs, B) between crenarchaeol and the BIT index and C) between summed brGDGTs and the BIT index for both concentrations (μg/g OC) and accumulation rates ($\mu g/cm^2/yr$). Red and blue lines indicate linear and log relationships for whole dataset, respectively.

Fig. 6. Detailed comparison of A) accumulation rates of summed brGDGTs (μg/cm^2/yr), B) accumulation rates of crenarchaeol (μg/cm^2/yr), and C) BIT index with D) historical flood records at Arles in France (Pichard, 1995) for the Roustan lobe period. Filled triangles indicate age control points.

Table 1

SPM samples and sites along the Rhône River and information.

Stations	Code	Location	Longitude (E)	Latitude (N)	Sampling date (dd/mm/yyyy)	River water depth (m)	Sampling water depth (m)	SPM (mg/l)	SPM OC (wt. %)
RW1	ST1-F4	Rhône River	4.64	43.77	18/05/2010	7.4	0	25.2	1.9
RW1	ST1-F3	Rhône River	4.64	43.77	18/05/2010	7.4	4	23.0	2.6
RW2	ST2-F7	Rhône River	4.62	43.68	19/05/2010	11	0	23.0	2.2
RW2	ST2-F5	Rhône River	4.62	43.68	19/05/2010	11	11	23.9	2.5
RW3	ST4-F17	Rhône River	4.74	43.49	20/05/2010	6	0	21.3	2.2
RW3	ST4-F18	Rhône River	4.74	43.49	20/05/2010	6	6	20.2	2.0
RW4	ST3-F15	Rhône River	4.85	43.33	20/05/2010	8	0	11.8	2.0
RW4	ST3-F13	Mixing zone	4.85	43.33	20/05/2010	8	3	14.5	1.9
RW4	ST3-F12	Mixing zone	4.85	43.33	20/05/2010	8	5	13.8	1.8
RW4	ST3-F9	Mixing zone	4.85	43.33	20/05/2010	8	8	17.5	1.9

Table 2

Linear regression analysis between crenarchaeol and summed brGDGTs, crenarchaeol and BIT index, and summed brGDGTs and BIT index for (A) concentrations (μg/g OC) and (B) accumulation rates (AR, μg/cm^2/yr). The relationship of $p < 0.05$ in significance level is highlighted in bold.

Parameters	Robes	Crenarchaeol vs. brGDGTs R^2	Crenarchaeol vs. brGDGTs p	Crenarchaeol vs. BIT R^2	Crenarchaeol vs. BIT p	BrGDGTs vs. BIT R^2	BrGDGTs vs. BIT p
A. Concentration							
	ROUSTAN	**0.37**	**<0.001**	**-0.46**	**<0.001**	0.003	0.69
	PÉGOULIER	0.15	0.40	-0.33	0.17	0.15	0.40
	GRAND RHÔNE	**0.30**	**0.01**	**-0.26**	**0.02**	0.15	0.09
	BRAS DE FER	-0.001	0.91	**-0.72**	**<0.001**	0.09	0.28
	Combined	**0.29**	**<.0001**	**-0.43**	**<.0001**	0.03	0.12
B. Accumulation rate							
	ROUSTAN	**0.50**	**<0.001**	**-0.26**	**<0.001**	0.01	0.43
	PÉGOULIER	0.06	0.61	-0.37	0.14	0.10	0.48
	GRAND RHÔNE	**0.31**	**0.01**	**-0.21**	**0.04**	0.19	0.05
	BRAS DE FER	0.04	0.44	**-0.64**	**<0.001**	**0.41**	**0.009**
	Combined	**0.59**	**<.0001**	**-0.15**	**0.0002**	0.03	0.09

Figure(s)

I

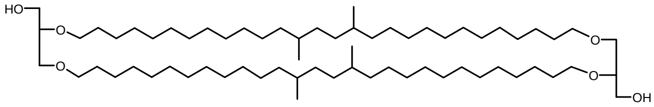

II

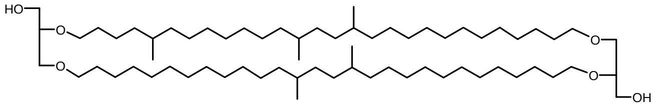

III

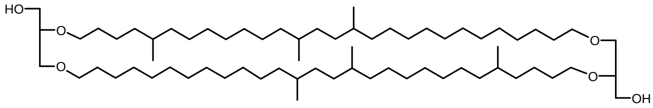

IV
Crenarchaeol

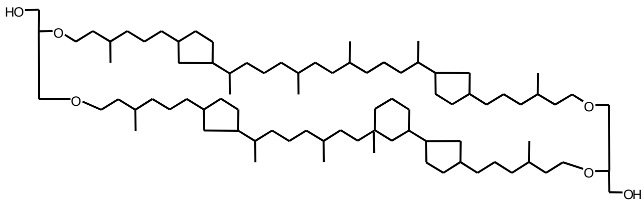

Fig. 1

Figure(s)

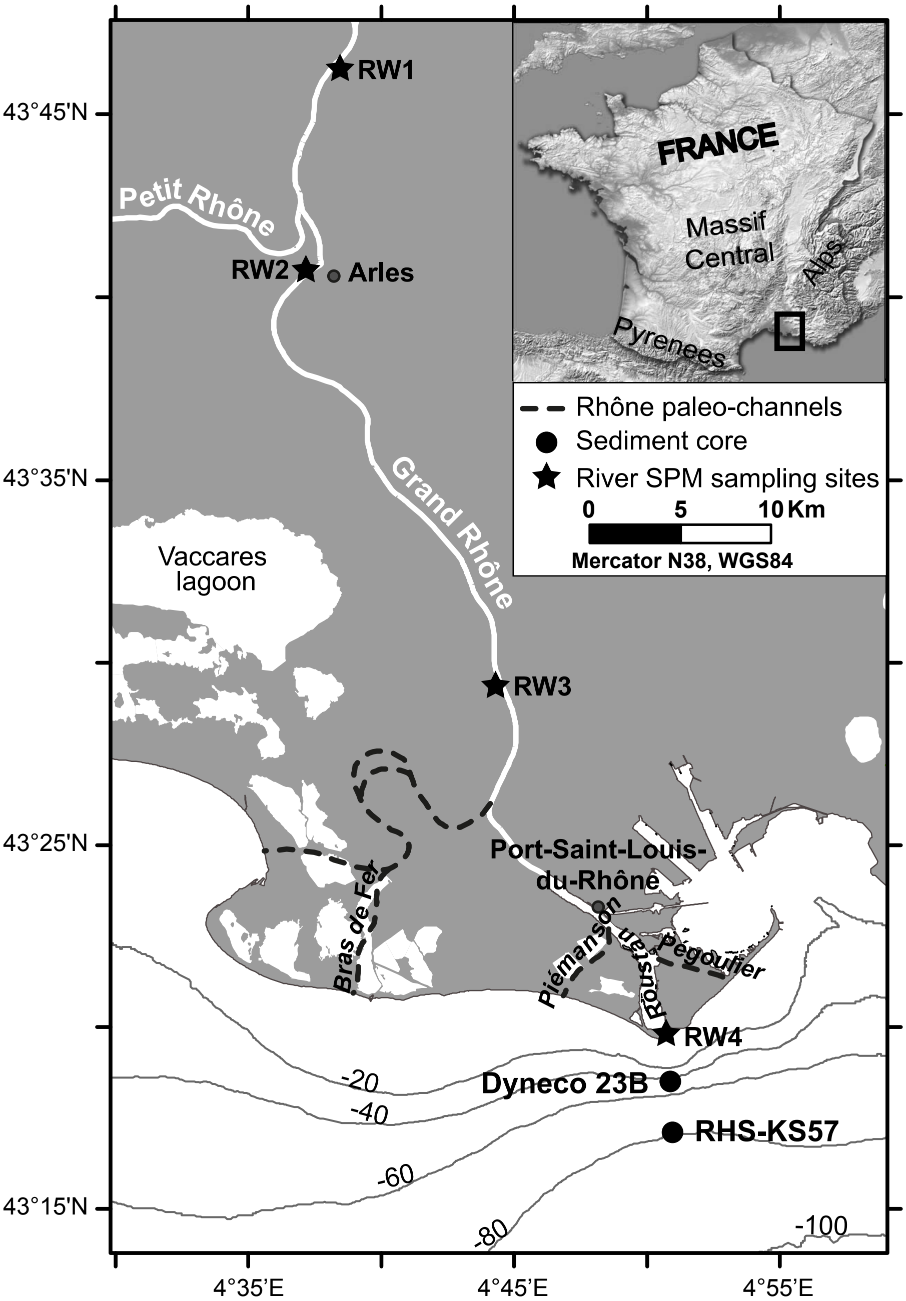

Fig. 2

Figure(s)

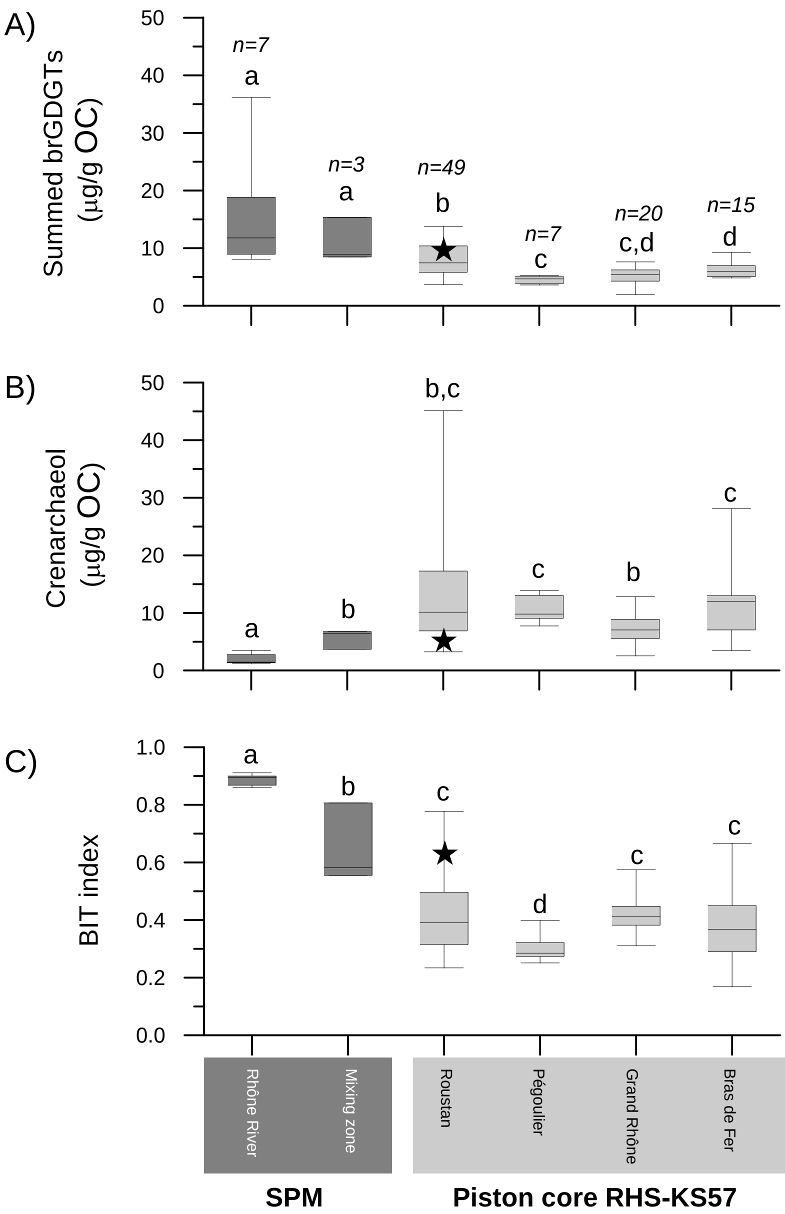

Fig. 3

Figure(s)

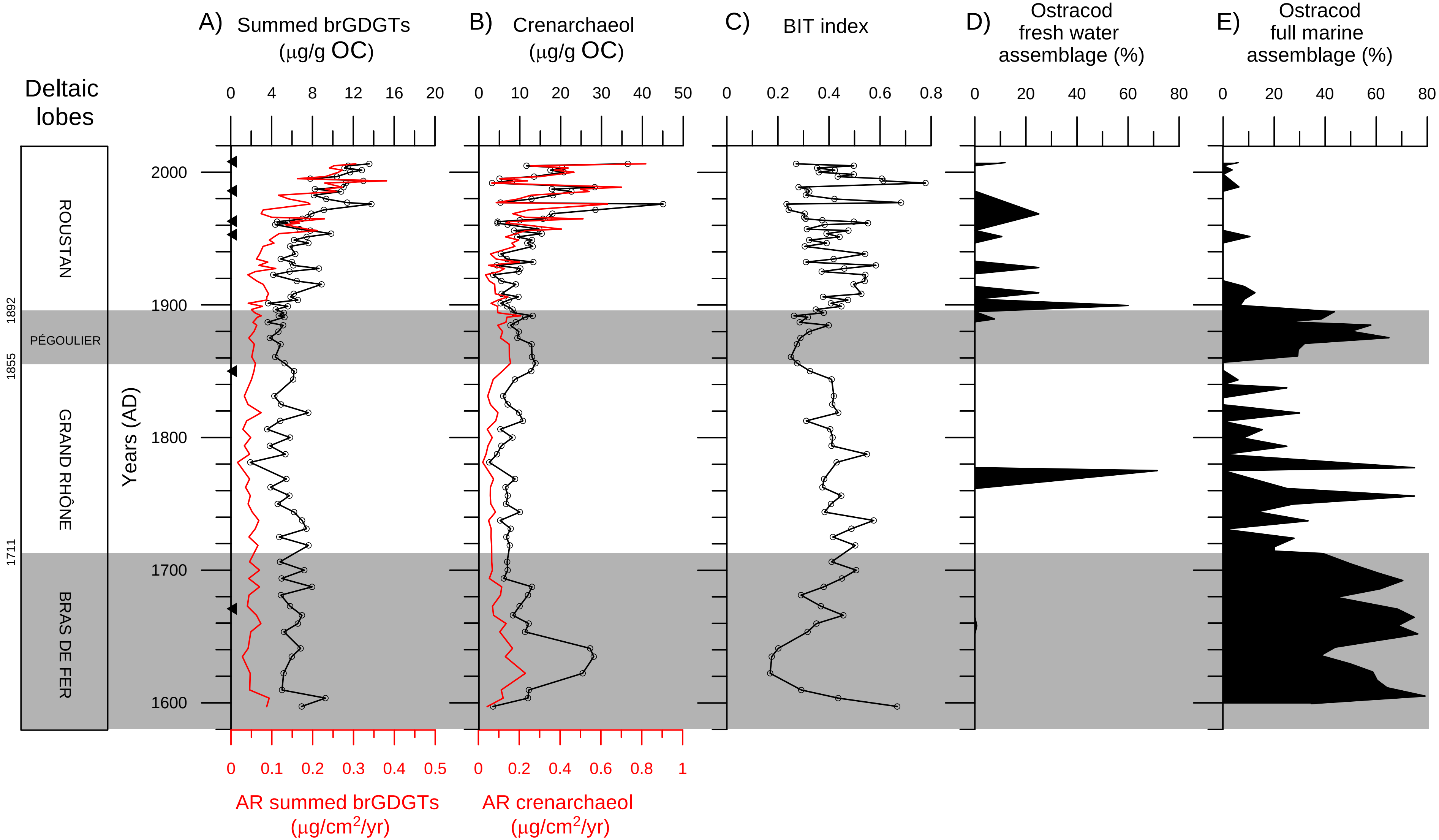

Fig. 4

Figure(s)

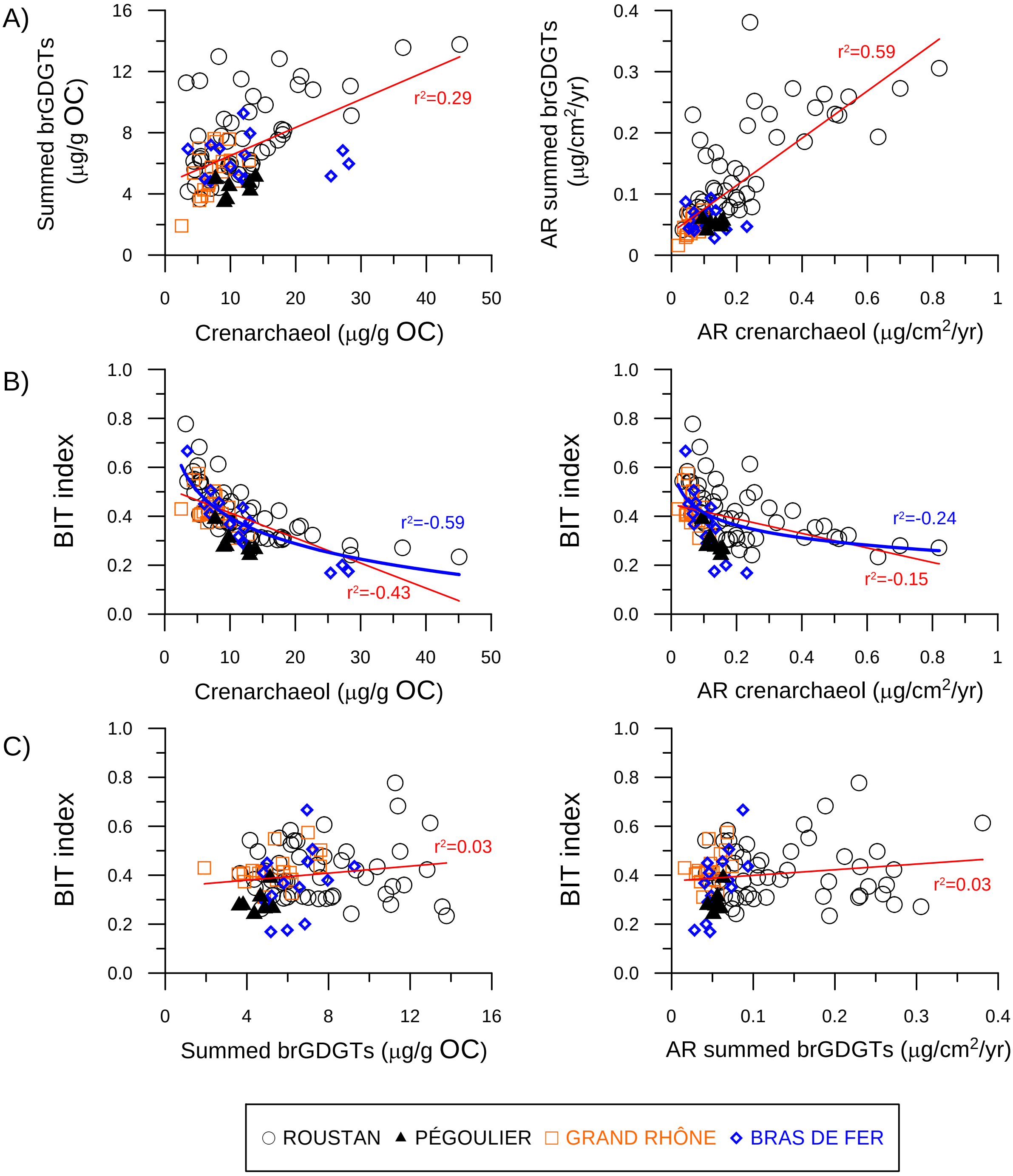

Fig. 5

Figure(s)

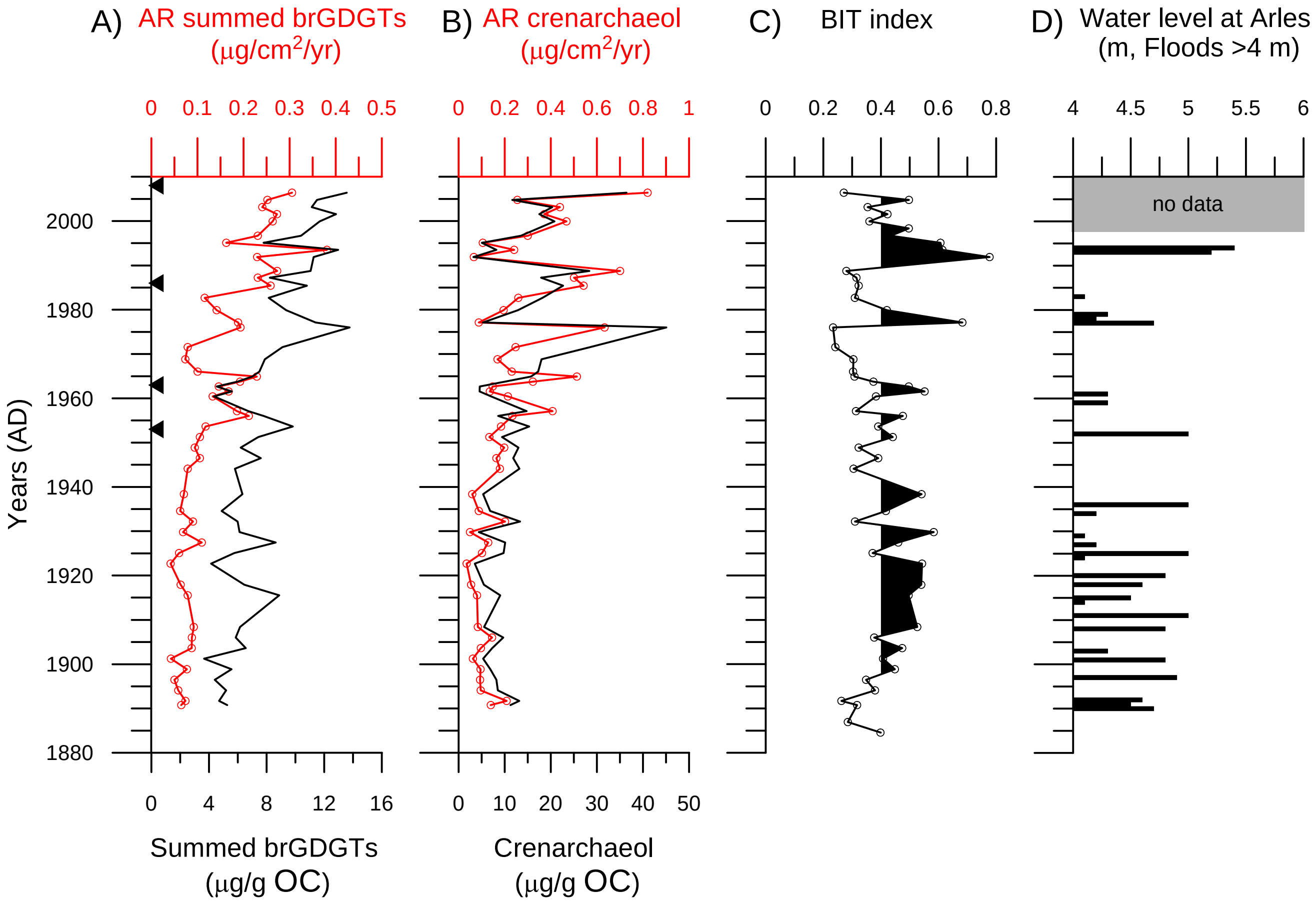

Fig. 6